Published in final edited form as:
Curr Biol. 2010 October 26; 20(20): 1840–1845. doi:10.1016/j.cub.2010.09.012.

Cse1l is a negative regulator of CFTR-dependent fluid secretion

Michel Bagnat[1,2,*], **Adam Navis**[1], **Sara Herbstreith**[1], **Koroboshka Brand-Arzamendi**[2], **Silvia Curado**[2], **Sherif Gabriel**[3], **Keith Mostov**[4], **Jan Huisken**[2], and **Didier Y. R. Stainier**[2,*]

[1] Department of Cell Biology, Duke University Medical School, Durham, NC 27710, USA

[2] Department of Biochemistry & Biophysics, UCSF, San Francisco, CA 94158-2324, USA

[3] Cystic Fibrosis Pulmonary Research and Clinical Treatment Center, The University of North Carolina, NC 27599, USA

[4] Department of Anatomy, UCSF, San Francisco, CA 94143-2140, USA

Summary

Transport of chloride through the Cystic Fibrosis Transmembrane Conductance Regulator (CFTR) channel is a key step in regulating fluid secretion in vertebrates[1,2]. Loss of CFTR function leads to cystic fibrosis (CF)[1,3,4], a disease that affects the lungs, pancreas, liver, intestine and vas deferens. Conversely, un-controlled activation of the channel leads to increased fluid secretion and plays a major role in several diseases and conditions including cholera[5,6] and other secretory diarrheas [7] as well as Polycystic Kidney Disease (PKD)[8–10]. Understanding how CFTR activity is regulated *in vivo* has been limited by the lack of a genetic model. Here, we used a forward genetic approach in zebrafish to uncover CFTR regulators. We report the identification, isolation and characterization of a mutation in the zebrafish *cse1l* gene that leads to the sudden and dramatic expansion of the gut tube. We show that this phenotype results from a rapid accumulation of fluid due to the un-controlled activation of the CFTR channel. Analyses in zebrafish embryos and mammalian cells indicate that Cse1l is a negative regulator of CFTR-dependent fluid secretion. This work demonstrates the importance of fluid homeostasis in development and establishes the zebrafish as a much needed model system to study CFTR regulation *in vivo*.

Results and Discussion

Following a genetic screen designed to identify mutants with defects in gut, liver or pancreas organogenesis[11], we identified a recessive mutation, *s866* (22.4% penetrance, n=548), which causes a striking gut phenotype. In *s866* mutants, internal organs appear to develop normally until 96–100 hours post fertilization (hpf) at which time the gut tube undergoes a process of expansion that results in a dramatically enlarged fluid-filled tube (Fig. 1). We named this mutant *baobab* (*bao*), after the African tree that accumulates water in its trunk. Using confocal microscopy, we observed that *bao*^{s866} mutants develop a very flat epithelium (devoid of folds) lining the lumen of this enlarged intestinal tube (Fig. 1A–E). Occasionally, delaminating cells were observed. However, *bao*^{s866} mutants still exhibit gut peristalsis and

[*] m.bagnat@cellbio.duke.edu; didier.stainier@ucsf.edu.

Supplemental Data

Supplemental Data include Supplemental Experimental Procedures and four supplemental figures.

the intestinal cells retain apical membrane polarity, cadherin localization, tight junctions, and basal laminin deposition (not shown). Using transmission electron microscopy (TEM), we observed a dramatic reduction in cell height and microvilli length in *bao*^{s866} mutant enterocytes (Fig. 1D–E). Nevertheless, *bao*^{s866} mutant enterocytes retain expression and localization of the absorptive cell marker 4e8[12] (Supp. Fig. 1A). Although all delaminating cells in *bao*^{s866} mutants appeared to undergo apoptosis, we did not observe a significant increase in apoptosis in mutants compared to WT (Sup. Fig. 1B). *bao*^{s866} mutants also exhibit exocrine pancreas degeneration and liver growth arrest after 96 hpf (Sup. Fig. 1C). To define the events leading to gut lumen expansion in *bao*^{s866} mutants, we first imaged the process from 96 to 120 hpf in larvae expressing Histone2A:GFP[13] using Selective Plane Illumination Microscopy (SPIM)[14]. This approach allowed us to visualize the shape and size of the gut tube and follow cell divisions. In WT larvae, the gut showed only a relatively small (46%) and steady increase in tube diameter between 96 and 120 hpf (Fig. 1H). Gut tube growth in WT was mostly due to cell divisions, increased folding of the epithelium and an increase in cell height associated with enterocyte polarization (see also Fig. 1B–C) but not to changes in luminal volume. In contrast, lumen expansion in the mutant was dramatic (511%) and rapid, taking place in approximately 200 minutes, and without cell division (Fig. 1F–G).

Next, we investigated the causes of gut lumen expansion in *bao*^{s866} mutants. At the tissue level, this phenotype is reminiscent of what occurs in the gut of mice exposed to cholera toxin[5], where the lumen is greatly enlarged by the CFTR-dependent accumulation of fluid[9]. CFTR is a vertebrate-specific gene[1]. Zebrafish CFTR shows a 55% identity and 75% similarity to human CFTR and is highly expressed in the gut by 4 dpf (see below and A.N. & M.B. unpublished). To test whether lumen expansion in *bao*^{s866} mutants was CFTR-dependent, we treated WT and mutant larvae with CFTR inhibitors from 72 to 120 hpf. Various CFTR inhibitors (Glibenclamide, CFTR172 and T08) effectively reduced the appearance of severely enlarged guts in *bao*^{s866} mutants (84% reduction for 5 μM T08, a CFTR172 analogue[10], n=1017 in total, 242 mutants)(Fig. 2A). In addition, treatment of *bao*^{s866} mutants with the CFTR inhibitor T08 significantly increased enterocyte height and microvilli length to levels close to WT (Supp. Fig. 4). Although the CFTR inhibitors blocked lumen expansion, they did not prevent cell delamination, suggesting that cell delamination/apoptosis and lumen expansion are two separable phenotypes.

We next investigated the effects of CFTR activation. Soaking 120 hpf WT larvae in water containing a specific CFTR activator[15] (15 μM CFTR-Act9) led to a robust and reversible accumulation of fluid, resulting in a dramatic expansion of the gut lumen and the flattening of enterocytes in half of the larvae (50.8%, n=360)(Fig. 2Bi; Supp. Fig. 2). This response had very similar kinetics and appearance (i.e. reduction in cell height and microvilli length) to those observed upon lumen expansion in *bao*^{s866} mutants, but did not cause cell delamination (Fig. 2Bii; Supp. Fig. 4). Altogether, our data indicate that the increase in lumen size observed in *bao*^{s866} mutants results from the un-controlled, CFTR-dependent accumulation of fluid in the gut lumen. Because the *bao*^{s866} mutation is recessive, it follows that Bao is a negative regulator of CFTR-dependent fluid secretion.

Since CFTR is regulated at multiple levels, including transcriptional and post transcriptional stages, it is possible that the increased CFTR activity observed in *bao*^{s866} mutants is due to increased expression and/or differences in subcellular localization of the channel. To investigate these possibilities, we raised an antibody against zebrafish CFTR. In western blots it recognized a protein of approximately 190 Kda (Supp. Fig. 3A). Importantly, the signal was dramatically reduced in extracts prepared from larvae injected with an anti-sense morpholino against CFTR compared to un-injected controls (Supp. Fig. 3A), indicating that the antibody recognizes CFTR specifically. In transverse sections, the antibody stained the

apical surface of gut epithelial cells (Sup. Fig. 3B). Western blot and immunohistological analyses revealed that CFTR protein levels or localization were not significantly different in *bao*^{s866} mutants compared to WT (Fig. 2C). These data suggest that Bao regulates CFTR-dependent fluid secretion by controlling CFTR activity and rule out transcriptional regulation, changes in CFTR steady state levels or subcellular distribution. However, we cannot exclude the possibility that differences in CFTR recycling[16], which would be very difficult to discern in vivo, also contribute to the increase in CFTR activity observed in *bao*^{s866} mutants.

To gain molecular insight into the cellular processes controlled by the Bao protein, we undertook a positional cloning project to isolate the corresponding gene. Using standard genetic mapping techniques, we defined a critical genomic interval on chromosome 12 containing only two genes, chromosome segregation 1-like (*cse1l*) and protein tyrosine phosphatase receptor gamma (*ptprg*)(Fig. 3A). Next, we isolated cDNAs from WT and mutant larvae for both genes. Sequencing of these cDNAs revealed the absence of exon 16 in the middle of the *cse1l* transcript that leads to a predicted premature stop codon in the next exon (Fig. 3B–C). No mutations were found in the *ptprg* cDNA. Genomic DNA sequencing revealed a T to A mutation upstream of exon 16's splice acceptor site (Fig. 3B). We confirmed the aberrant splicing of exon 16 in the mutant by reverse transcriptase PCR on pools of RNA made from *bao*^{s866} mutants and WT siblings (Fig. 3C). Cse1l was depleted in extracts prepared from *bao*^{s866} mutants compared to WT siblings as judged by immunoblots using antibodies against the N-terminus of human CSE1L (Fig. 3Di). However, we could not unequivocally detect the predicted truncated form of the protein in extracts made from *bao*^{s866} mutants due to the presence of a cross-reacting protein of the same size (asterisk in Fig. 3Di). To determine whether the mutant cDNA produces a truncated protein, we transfected HEK293 cells and performed an immunoblot analysis. The mutant cDNA produced a polypeptide of approximately 60 KDa, in agreement with the size prediction inferred from cDNA sequencing (Fig. 3Dii).

Next, we knocked down the expression of Cse1l and Ptprg using anti-sense morpholinos. Knock down of Cse1l (Fig. 3Ei) but not Ptprg (not shown) phenocopied *bao*^{s866}. Immunoblot analysis confirmed that the phenotype of the *cse1l* morphants showed a good correlation with the level of Cse1l depletion (Fig. 3Eii). To determine the pattern of *cse1l* expression, we performed an in situ hybridization (ISH) analysis during WT development. The *cse1l* transcript was present at the 2-cell stage (Fig. 3F), indicating that it is maternally provided. Expression was broad early on but became restricted to the endoderm and parts of the brain by 48 hpf. At 96 hpf *cse1l* was strongly expressed in the gut, liver and exocrine pancreas and parts of the brain and retina (Fig. 3F). Expression was strongest in the gut after 96 hpf, coinciding with the onset of the gut expansion phenotype. Thus, the expression pattern of *cse1l* shows a good correlation with the *bao*^{s866} phenotype, affecting mostly gut, liver and pancreas. To determine the subcellular localization of the Cse1l protein, we stained sections of 120 hpf WT larvae. At 120 hpf, Cse1l was found enriched in the gut and liver where we also found expression by ISH. The protein localized to the sub-apical and apical region of gut enterocytes and was also found associated with lateral and basal membranes (Fig. 3G). Altogether our data indicate that *bao* corresponds to *cse1l*.

Cse1l was originally isolated in a screen looking for regulators of chromosome segregation (hence the name) in yeast[17]. This highly conserved (86% identity, 93% similarity between zebrafish and humans) and essential gene[18] has been implicated in apoptosis[19], nuclear-cytoplasmic transport[20], cell-cell adhesion[21] and chromatin regulation[22]. Therefore, it seems very likely that the cell delamination/apoptosis phenotype in *bao*^{s866} mutants is linked to the nuclear and lateral membrane functions of Cse1l. However, the role of Cse1l in regulating CFTR-dependent fluid secretion is clearly separable from other functions (Fig.

2Aii). Moreover, zebrafish mutations in the nucleoporin gene *elys* trigger apoptosis in the gut but not fluid accumulation[23,24]. Our data suggest a functional interaction between Cse1l and CFTR. To test whether these two proteins also interact physically, we performed co-immunoprecipitation experiments in HEK293 cells expressing human HA-tagged CFTR (CFTR-HA)[25] and GFP-Cse1l or GFP-Cse1l^{s866} respectively. Notably, CFTR-HA co-immunoprecipitated with GFP-Cse1l but showed a much weaker interaction with GFP-Cse1l^{s866} (Fig. 4Ai). At the immunofluorescence level, a fraction of GFP-Cse1l co-localized with CFTR-HA (Fig. 4Aii). We also co-immunoprecipitated endogenous CFTR and Cse1l from human intestinal Caco-2 cells (not shown). Interestingly, a recent mass spectrometric analysis of CFTR-associated proteins identified CSE1L among several other potential CFTR partners in various human cell lines[26].

To investigate whether Cse1l regulates fluid secretion in mammalian cells, we employed a clone of Madin-Darby Canine Kidney (MDCK) cells that expresses endogenous CFTR (MDCK-C7)[27] and performed 3D cultures. When grown in Matrigel^{TM}, these cells form hollow cysts that exhibit forskolin-stimulated, CFTR-dependent fluid transport and lumen expansion[9,28]. Forskolin addition increases intracellular cAMP levels and stimulates protein kinase A which in turn activates the CFTR channel through phosphorylation[29]. To test the effect of Cse1l over-expression and knockdown we made stable MDCKC7 lines over-expressing GFP-tagged WT and mutant zebrafish Cse1l (GFP-Cse1l and GFP-Cse1l^{s866} respectively) and examined the response to forskolin in 3D cultures. Cse1l is highly conserved between zebrafish and mammals and the fish protein can functionally substitute for the mammalian protein (see below). Interestingly, while addition of forskolin (1 μM for 16 hrs) led to a robust (25% increase in diameter or close to 200% increase in volume) and significant ($p<0.00001$, n=161) enlargement of control (vector only) or GFP-Cse1l^{s866} expressing cysts, it did not affect the size of GFP-Cse1l expressing cysts ($p=0.695$, n=131) (Fig. 4). It is important to note that while cysts made from cells transfected with vector only or GFP-Cse1l^{s866} possessed mostly very thin (stretched) cells surrounding a single large lumen (100 μm on average), GFP-Cse1l-expressing cysts were mostly multi-layered and contained multiple small lumens (1–10 μm). Thus, the difference in luminal volume was in fact much greater than the 200% increase derived from measurements of cyst diameter. Next, we knocked down (more than 80%) endogenous Cse1l expression using lentivirus-mediated expression of short hairpin interfering RNAs (sh-RNAs) (Fig. 4Ci). The DNA sequence differences between zebrafish and dog Cse1l make the zebrafish construct insensitive to the sh-RNAs. (Fig. 4Ci). Upon Cse1l knockdown we observed a robust (48% increase in diameter or more than 300% increase in total cyst volume) and significant ($p<0.00001$, n=200) expansion of the lumen that could be blocked by GFP-Cse1l expression ($p=0.643$, n=149). Finally, we assayed CFTR activity in HEK293 cells expressing CFTR by using a halide-sensitive YFP variant (YFP-H148Q)[30] and found that Cse1l over-expression strongly inhibited CFTR activity (Supp. Fig. 4). Together, these experiments suggest that Cse1l is a negative regulator of CFTR activity in mammalian cells.

Altogether, our results are consistent with a scenario in which binding of Cse1l to CFTR results in the inhibition of the channel. Alternatively, Cse1l may be required for the function of a CFTR inhibitor. While we cannot exclude an effect on the activity of other channels or channel cross regulation, the physical interaction of Cse1l with CFTR suggests that Cse1l regulates CFTR activity directly.

Studies of CFTR function have relied mostly on cell culture and genetic association studies of populations of CF patients. While these studies have provided very valuable insights, an in vivo correlate has not yet been established. This work establishes zebrafish as a forward genetics model system to study CFTR biology and demonstrates that these studies are translatable to mammalian models.

Highlights

- Regulation of CFTR activity is critical during zebrafish gut development
- Loss of Cse1l function leads to the un-controlled activation of the CFTR channel
- Cse1l is a negative regulator of CFTR-dependent fluid secretion
- Forward genetics in zebrafish allows the isolation of CFTR regulators

Supplementary Material

Refer to Web version on PubMed Central for supplementary material.

Acknowledgments

We thank Brigid Hogan, Ken Poss, Christopher Penland and Çagla Eroglu for critically reading the manuscript, and Alan Verkman for discussions and reagents. We are grateful to G. Lukacs, M. Gentzch, P. Haggie and J. Riordan for reagents and constructs. M.B. was supported by an EMBO long-term postdoctoral fellowship, J.H. by a Human Frontier Science Program postdoctoral fellowship. This work was funded in part by grant 0810 from the Cystic Fibrosis Foundation (CFF) and an NIH Innovator Award (1DP2OD006486) to M.B., the NIH (DK067153 and DK074398 to K.M.; P30 DK065988 to S.G.; DK60322 and DK075032 to D.Y.R.S.) as well as the CFF and Packard Foundation (D.Y.R.S.) .

References

1. Riordan JR. CFTR function and prospects for therapy. Annu Rev Biochem. 2008; 77:701–726. [PubMed: 18304008]
2. Brown PD, Davies SL, Speake T, Millar ID. Molecular mechanisms of cerebrospinal fluid production. Neuroscience. 2004; 129:957–970. [PubMed: 15561411]
3. Riordan JR, Rommens JM, Kerem B, Alon N, Rozmahel R, Grzelczak Z, Zielenski J, Lok S, Plavsic N, Chou JL, et al. Identification of the cystic fibrosis gene: cloning and characterization of complementary DNA. Science. 1989; 245:1066–1073. [PubMed: 2475911]
4. Anderson MP, Gregory RJ, Thompson S, Souza DW, Paul S, Mulligan RC, Smith AE, Welsh MJ. Demonstration that CFTR is a chloride channel by alteration of its anion selectivity. Science. 1991; 253:202–205. [PubMed: 1712984]
5. Gabriel SE, Brigman KN, Koller BH, Boucher RC, Stutts MJ. Cystic fibrosis heterozygote resistance to cholera toxin in the cystic fibrosis mouse model. Science. 1994; 266:107–109. [PubMed: 7524148]
6. Verkman AS, Lukacs GL, Galietta LJ. CFTR chloride channel drug discovery--inhibitors as antidiarrheals and activators for therapy of cystic fibrosis. Curr Pharm Des. 2006; 12:2235–2247. [PubMed: 16787252]
7. McCole DF, Barrett KE. Epithelial transport and gut barrier function in colitis. Curr Opin Gastroenterol. 2003; 19:578–582. [PubMed: 15703608]
8. Sullivan LP, Wallace DP, Grantham JJ. Chloride and fluid secretion in polycystic kidney disease. J Am Soc Nephrol. 1998; 9:903–916. [PubMed: 9596091]
9. Li H, Findlay IA, Sheppard DN. The relationship between cell proliferation, Cl- secretion, and renal cyst growth: a study using CFTR inhibitors. Kidney Int. 2004; 66:1926–1938. [PubMed: 15496164]
10. Yang B, Sonawane ND, Zhao D, Somlo S, Verkman AS. Small-molecule CFTR inhibitors slow cyst growth in polycystic kidney disease. J Am Soc Nephrol. 2008; 19:1300–1310. [PubMed: 18385427]
11. Ober EA, Verkade H, Field HA, Stainier DY. Mesodermal Wnt2b signalling positively regulates liver specification. Nature. 2006; 442:688–691. [PubMed: 16799568]

12. Crosnier C, Vargesson N, Gschmeissner S, Ariza-McNaughton L, Morrison A, Lewis J. Delta-Notch signalling controls commitment to a secretory fate in the zebrafish intestine. Development. 2005; 132:1093–1104. [PubMed: 15689380]
13. Pauls S, Geldmacher-Voss B, Campos-Ortega JA. A zebrafish histone variant H2A.F/Z and a transgenic H2A.F/Z:GFP fusion protein for in vivo studies of embryonic development. Dev Genes Evol. 2001; 211:603–610. [PubMed: 11819118]
14. Huisken J, Swoger J, Del Bene F, Wittbrodt J, Stelzer EH. Optical sectioning deep inside live embryos by selective plane illumination microscopy. Science. 2004; 305:1007–1009. [PubMed: 15310904]
15. Ma T, Vetrivel L, Yang H, Pedemonte N, Zegarra-Moran O, Galietta LJ, Verkman AS. High-affinity activators of cystic fibrosis transmembrane conductance regulator (CFTR) chloride conductance identified by high-throughput screening. J Biol Chem. 2002; 277:37235–37241. [PubMed: 12161441]
16. Gentzsch M, Chang XB, Cui L, Wu Y, Ozols VV, Choudhury A, Pagano RE, Riordan JR. Endocytic trafficking routes of wild type and DeltaF508 cystic fibrosis transmembrane conductance regulator. Mol Biol Cell. 2004; 15:2684–2696. [PubMed: 15075371]
17. Xiao Z, McGrew JT, Schroeder AJ, Fitzgerald-Hayes M. CSE1 and CSE2, two new genes required for accurate mitotic chromosome segregation in Saccharomyces cerevisiae. Mol Cell Biol. 1993; 13:4691–4702. [PubMed: 8336709]
18. Bera TK, Bera J, Brinkmann U, Tessarollo L, Pastan I. Cse1l is essential for early embryonic growth and development. Mol Cell Biol. 2001; 21:7020–7024. [PubMed: 11564884]
19. Behrens P, Brinkmann U, Wellmann A. CSE1L/CAS: its role in proliferation and apoptosis. Apoptosis. 2003; 8:39–44. [PubMed: 12510150]
20. Kutay U, Bischoff FR, Kostka S, Kraft R, Gorlich D. Export of importin alpha from the nucleus is mediated by a specific nuclear transport factor. Cell. 1997; 90:1061–1071. [PubMed: 9323134]
21. Jiang MC, Liao CF, Tai CC. CAS/CSE 1 stimulates E-cadhrin-dependent cell polarity in HT-29 human colon epithelial cells. Biochem Biophys Res Commun. 2002; 294:900–905. [PubMed: 12061792]
22. Tanaka T, Ohkubo S, Tatsuno I, Prives C. hCAS/CSE1L associates with chromatin and regulates expression of select p53 target genes. Cell. 2007; 130:638–650. [PubMed: 17719542]
23. de Jong-Curtain TA, Parslow AC, Trotter AJ, Hall NE, Verkade H, Tabone T, Christie EL, Crowhurst MO, Layton JE, Shepherd IT, et al. Abnormal nuclear pore formation triggers apoptosis in the intestinal epithelium of elys-deficient zebrafish. Gastroenterology. 2009; 136:902–911. [PubMed: 19073184]
24. Davuluri G, Gong W, Yusuff S, Lorent K, Muthumani M, Dolan AC, Pack M. Mutation of the zebrafish nucleoporin elys sensitizes tissue progenitors to replication stress. PLoS Genet. 2008; 4:e1000240. [PubMed: 18974873]
25. Sharma M, Pampinella F, Nemes C, Benharouga M, So J, Du K, Bache KG, Papsin B, Zerangue N, Stenmark H, et al. Misfolding diverts CFTR from recycling to degradation: quality control at early endosomes. J Cell Biol. 2004; 164:923–933. [PubMed: 15007060]
26. Wang X, Venable J, LaPointe P, Hutt DM, Koulov AV, Coppinger J, Gurkan C, Kellner W, Matteson J, Plutner H, et al. Hsp90 cochaperone Aha1 downregulation rescues misfolding of CFTR in cystic fibrosis. Cell. 2006; 127:803–815. [PubMed: 17110338]
27. Lahr TF, Record RD, Hoover DK, Hughes CL, Blazer-Yost BL. Characterization of the ion transport responses to ADH in the MDCK-C7 cell line. Pflugers Arch. 2000; 439:610–617. [PubMed: 10764221]
28. Bagnat M, Cheung ID, Mostov KE, Stainier DY. Genetic control of single lumen formation in the zebrafish gut. Nat Cell Biol. 2007; 9:954–960. [PubMed: 17632505]
29. Hallows KR, Kobinger GP, Wilson JM, Witters LA, Foskett JK. Physiological modulation of CFTR activity by AMP-activated protein kinase in polarized T84 cells. Am J Physiol Cell Physiol. 2003; 284:C1297–1308. [PubMed: 12519745]
30. Galietta LJ, Haggie PM, Verkman AS. Green fluorescent protein-based halide indicators with improved chloride and iodide affinities. FEBS Lett. 2001; 499:220–224. [PubMed: 11423120]

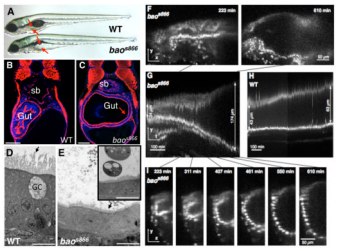

Figure 1. *bao*^{s866} mutants undergo a dramatic and rapid expansion of the gut lumen between 96 and 120 hpf

A: Brightfield image of 120 hpf WT and *bao*^{s866} mutant larvae. Arrows point to the edges of the gut lumen. **B–C:** Confocal images of cross-sections of 120 hpf WT (B) and *bao*^{s866} mutant (C). The arrow points to a delaminating cell. f-actin (red), DAPI (blue), sb: swimbladder. Scale bars: 50 μm. **D–E:** Dramatic shortening of microvilli (arrows) in *bao*^{s866} mutant enterocytes seen by TEM at 120 hpf. Remnants of apoptotic cells (insert) found in the lumen. GC: goblet cell. Scale bars: 10 μm. **F–I:** Rapid expansion of the gut lumen in *bao*^{s866} mutants expressing H2A:GFP. **F:** still images (lateral views) from a *bao*^{s866} mutant SPIM recording between (96–120 hpf) showing first and last frames. **G–H:** Kymographs from *bao*^{s866} mutant (G) and WT (H) gut. Lumen expansion in the mutant occurred in ~200 min, no cell division was observed. **I:** Still images (lateral views) from the *bao*^{s866} mutant SPIM recording corresponding to the kymograph shown in (G).

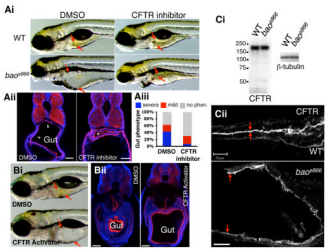

Figure 2. Lumen expansion in *bao*^{s866} mutants results from increased CFTR-dependent fluid secretion

A: Inhibition of CFTR blocks lumen expansion in *bao*^{s866} mutants. **Ai:** Brightfield images of WT and *bao*^{s866} mutants incubated with DMSO (0.1 %) or the CFTR inhibitor T08 (5 μM) from 72 to 120 hpf. Arrows point to the edges of the gut lumen. **Aii:** Confocal images of cross-sections of 144 hpf control and T08-treated *bao*^{s866} mutants. Arrowheads point to delaminating cells. f-actin (red), DAPI (blue). Scale bars: 50 μm. **Aiii:** Quantification of the gut phenotype in control and T08-treated *bao*^{s866} mutants. Larvae were placed in three phenotypic categories (no phenotype, mild or severe phenotype) and then genotyped. **B:** Activation of CFTR in WT phenocopies the gut lumen expansion defect of *bao*^{s866} mutants. **Bi:** Brighfield image of 144 hpf WT larvae treated with DMSO (0.15%) or CFTR-Act9 (15 μM). Arrows point to the edges of the gut lumen. **Bii:** Confocal images of cross-sections of 144 hpf control and CFTR-Act9-treated WT larvae. f-actin:red, DAPI:blue. Scale bars: 20 μm. **C:** CFTR expression and localization is not affected in *bao*^{s866} mutants compared to WT. **Ci:** Immunoblot of 120 hpf WT and *bao*^{s866} mutants probed against CFTR and β-tubulin. **Cii:** Confocal images of wholemounts of 120 hpf WT and *bao*^{s866} mutants stained for CFTR. The arrows point to the apical surface of the gut. Anterior to the right.

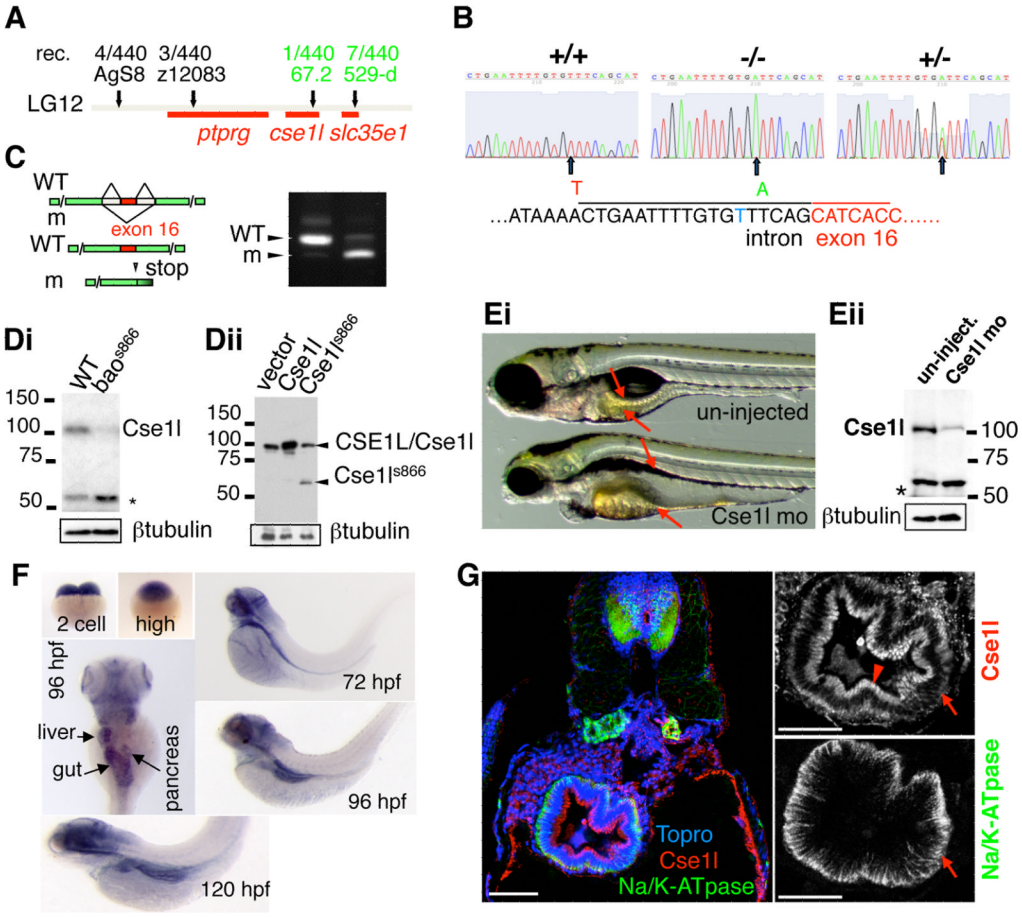

Figure 3. Isolation of the *bao* gene

A: Positional cloning of *bao*. The number of recombinants (rec.) for each marker is shown. **B:** sequencing of genomic DNA from +/+, −/− and +/− larvae revealed a T to A mutation (arrow) upstream of exon 16's splice acceptor site. **C:** RT-PCR on pools of RNA made from WT and *bao*^{s866} mutants demonstrates defective splicing of exon 16 in *bao*^{s866} mutants leading to a premature stop codon in exon 17. **Di:** Cse1l is depleted in *bao*^{s866} mutants. The asterisk marks the position of a cross-reacting protein band. **Dii:** The *bao*^{s866} mutation produces a truncated protein that can be detected in immunoblots of transfected HEK293 cells. **Ei:** Knockdown of Cse1l using an anti-sense morpholino targeting the translation start site phenocopies the *bao*^{s866} mutation (22% penetrance at 5 dpf, n=220). **Eii:** Immunoblot of 5 dpf un-injected and Cse1l morphants demonstrating knockdown of this protein. **F:** ISH analysis using an anti-sense probe directed against the 3' of the *cse1l* mRNA. **G:** Immunofluorescence on WT sections showing Cse1l in the sub-apical (arrowhead) and basolateral (arrow) regions of intestinal cells at 120 hpf. Scale bars: 50μm.

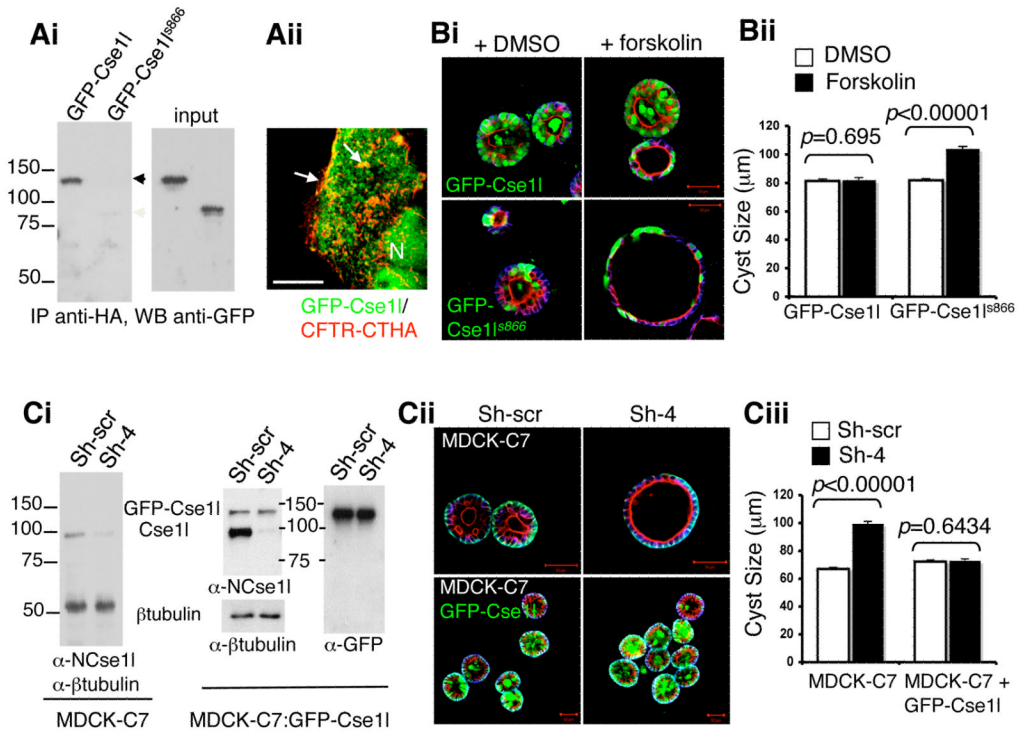

Figure 4. Cse1l negatively regulates fluid secretion in mammalian MDCK-C7 cells

Ai: zebrafish GFP-Cse1l but not GFP-Cse1l^{s866} co-immunoprecipitates with human CFTR-CTHA. **Aii:** partial co-localization (arrows) of GFP-Cse1l and CFTR-CTHA in transfected HEK293 cells. Scale bar=10μm; N, nucleus. **B:** Over-expression of zebrafish GFP-Cse1l abrogates the stimulatory effect of forskolin on CFTR-dependent fluid secretion in 3D cultures of mammalian MDCK-C7 cells. **Bi:** MDCK-C7 cells were grown on Matrigel^{TM} for 4 d and then forskolin (1 μM) was added for 16 hrs before the cysts were fixed and imaged. Green:GFP, red:f-actin, blue:β-catenin. Scale bars: 50μm. **Bii:** quantification of Bi (n=161 for GFP-Cse1l^{s866}; n=131 for GFP-Cse1l). Error bars: s.e.m. **C:** Depletion of Cse1l leads to increased fluid secretion in 3D cultures of MDCK-C7 cells. **Ci:** Immunoblot showing knockdown of dog Cse1l in Sh4 but not in control Sh-scr infected cells. **Cii:** Knockdown of dog Cse1l leads to lumen expansion in control but not in GFP-Cse1l-expressing MDCK-C7 cells in 3D cultures (5 d in Matrigel^{TM}) following forskolin treatment. red: f-actin; green:β-catenin (upper panels), GFP (lower panels); blue:Topro. Scale bars: 50 μm. **Ciii:** quantification of (Cii). n=200 for control; n=149 for GFP-Cse1l. Error bars: s.e.m.